



Updated BBN bounds on the cosmological lepton asymmetry for non-zero θ_{13}

Gianpiero Mangano^a, Gennaro Miele^{a,b}, Sergio Pastor^{c,*}, Ofelia Pisanti^{a,b}, Srdjan Sarikas^{b,d}

^a Istituto Nazionale di Fisica Nucleare, Sezione di Napoli, Complesso Universitario di Monte S. Angelo, I-80126 Napoli, Italy

^b Dipartimento di Scienze Fisiche, Università di Napoli Federico II, Complesso Universitario di Monte S. Angelo, I-80126 Napoli, Italy

^c Instituto de Física Corpuscular, CSIC-Universitat de València, Ed. Institutos de Investigación, Apdo. correos 22085, E-46071 Valencia, Spain

^d Max-Planck-Institut für Physik, Werner-Heisenberg-Institut, Föhringer Ring 6, 80802 München, Germany

ARTICLE INFO

Article history:

Received 4 January 2012

Accepted 6 January 2012

Available online 10 January 2012

Editor: S. Dodelson

Keywords:

Neutrinos

Physics of the early Universe

Primordial asymmetries

ABSTRACT

We discuss the bounds on the cosmological lepton number from Big Bang Nucleosynthesis (BBN), in light of recent evidences for a large value of the neutrino mixing angle θ_{13} , $\sin^2 \theta_{13} \gtrsim 0.01$ at 2σ . The largest asymmetries for electron and μ , τ neutrinos compatible with ${}^4\text{He}$ and ${}^2\text{H}$ primordial yields are computed versus the neutrino mass hierarchy and mixing angles. The flavour oscillation dynamics is traced till the beginning of BBN and neutrino distributions after decoupling are numerically computed. The latter contains in general, non-thermal distortion due to the onset of flavour oscillations driven by solar squared mass difference in the temperature range where neutrino scatterings become inefficient to enforce thermodynamical equilibrium. Depending on the value of θ_{13} , this translates into a larger value for the effective number of neutrinos, N_{eff} . Upper bounds on this parameter are discussed for both neutrino mass hierarchies. Values for N_{eff} which are large enough to be detectable by the Planck experiment are found only for the (presently disfavoured) range $\sin^2 \theta_{13} \leq 0.01$.

© 2012 Elsevier B.V. All rights reserved.

1. Introduction

Nowadays flavour neutrino oscillations are well established thanks to a plethora of experimental results on the detection of reactor, accelerator, atmospheric and solar neutrinos. Two neutrino mass-squared differences and three mixing angles drive oscillations among the three active neutrinos, all of them, except one angle, known with a precision better than 25% [1–3]. The last parameter which is not so well known is the mixing angle θ_{13} . Until very recently only an upper bound on $\sin^2 \theta_{13}$ existed, while the present year we have witnessed the first indications of non-zero θ_{13} values from the analysis of global data [2,3], especially recent $\nu_{\mu} \rightarrow \nu_e$ searches at the T2K long-baseline experiment [4]. This result opens up the possibility of measuring, in a not so distant future, the pattern of neutrino masses (the mass hierarchy) and a possible CP violation in the leptonic sector [5], the last remaining unknowns together with the nature of neutrinos (Dirac or Majorana).

Neutrino oscillations have implications in many research areas in particle and astroparticle physics. However, the consequences of non-zero neutrino mixing in cosmology are not so important, despite the fact that relic neutrinos are the second most abundant particles in the Universe, with almost the same number den-

sity as photons. The reason is well known: in first approximation all neutrino flavours were produced by frequent interactions in the early hot Universe, with the same momentum spectra. Thus neutrino oscillations, although effective right after neutrino decoupling, do not modify the properties of cosmological neutrinos (except for very small effects from non-instantaneous neutrino decoupling [6]). This holds for active neutrino oscillations, while the case of active–sterile oscillations does lead to effects on cosmological observables if one or more extra neutrino species are populated (see e.g. [7–10]).

There exists, however, one situation where active–active oscillations have an impact on cosmological neutrinos, namely when a large flavour neutrino asymmetry was previously created. It is usually assumed that such an asymmetry, parameterized by the number density ratios

$$\eta_{\nu\alpha} = \frac{n_{\nu\alpha} - n_{\bar{\nu}\alpha}}{n_{\gamma}}, \quad \alpha = e, \mu, \tau, \quad (1)$$

should be of the same order of the cosmological baryon number $\eta_b = (n_b - n_{\bar{b}})/n_{\gamma}$, due to the equilibration by sphalerons of lepton and baryon asymmetries in the very early Universe. Thus one does not expect flavour neutrino asymmetries much larger than a few times 10^{-10} , the value of η_b measured by present observations, such as 7-year data from the WMAP satellite and other cosmological measurements [11]. There are, however, some models where a lepton asymmetry orders of magnitude larger than the baryon one could survive, see e.g. [12,13], in the neutrino sector with an

* Corresponding author.

E-mail address: pastor@ific.uv.es (S. Pastor).

influence on fundamental physics in the early Universe, such as the QCD transition [14] or a potential relation with the cosmological magnetic fields at large scales [15].

Present cosmological observations are not sensitive to a large neutrino asymmetry if $|\eta_{\nu}| \lesssim 10^{-2}$. Only larger values lead to a significant enhancement of the contribution of active neutrinos to the radiation energy density of the Universe or to changes in the production of light elements in Big Bang Nucleosynthesis (BBN). In particular, the primordial abundance of ${}^4\text{He}$ depends on the presence of an electron neutrino asymmetry and sets a stringent bound on η_{ν_e} which does not apply to the other flavours unless neutrino oscillations are effective before BBN, leaving a total neutrino asymmetry of order unity unconstrained [16,17].

A decade ago, it was shown that flavour neutrino conversions in the early Universe are indeed suppressed by matter effects at large temperatures, and it is only at temperatures $T \lesssim 10$ MeV that oscillations set on and are large enough to achieve strong flavor conversions before BBN [18–21]. For the present measured values of neutrino mixing parameters, the degree of flavour equilibration depends on the value of θ_{13} . As discussed in [22], this parameter fixes the onset of flavour oscillations involving ν_e 's, which in turn determines whether neutrinos interact enough with electrons and positrons to transfer the excess of energy density due to the initial η_{ν_α} to the electromagnetic plasma. Recently we have found the BBN bounds on the cosmological lepton number for a range of initial flavour neutrino asymmetries [23].

Prompted by the recent indication of non-zero values for θ_{13} and the hints of possible extra radiation from cosmological data [11], we have updated the analysis in [23] with the aim of finding the BBN bounds on both the total neutrino asymmetry and its maximum contribution to the radiation content of the Universe in the whole range of θ_{13} values allowed by oscillation data, as well as considering both neutrino mass hierarchies.

This Letter is organized as follows. We introduce in Section 2 the formalism of kinetic equations which rule the evolution of neutrino distributions and describe the dynamics of neutrino asymmetries in the epoch just immediately BBN. In Section 3 we study the BBN constraints on lepton number that can be obtained for a wide range of initial neutrino asymmetries, with emphasis on the effects of a mixing angle θ_{13} in the region experimentally favoured. Finally in Section 4 we give our concluding remarks.

2. Neutrino evolution in the presence of lepton asymmetries

Active neutrinos were produced in the very early Universe and their energy spectrum is kept in chemical and kinetic equilibrium by weak interactions until temperatures $T \simeq \mathcal{O}$ (MeV), when the corresponding collision rates fall below the cosmological expansion rate. Therefore, if flavour neutrino asymmetries existed, at larger temperatures the neutrino distribution of momenta is a Fermi–Dirac spectrum parameterized by a temperature T (the same of e^+e^- and photons) and a well defined chemical potential μ_{ν_α} for $\alpha = e, \mu, \tau$. Each flavor neutrino asymmetry in Eq. (1) can be expressed in terms of the corresponding degeneracy parameter $\xi_\alpha \equiv \mu_{\nu_\alpha}/T$ as

$$\eta_{\nu_\alpha} = \frac{1}{12\zeta(3)} (\pi^2 \xi_\alpha + \xi_\alpha^3), \quad (2)$$

with $\zeta(3) \simeq 1.20206$. This expression is modified later by a factor $(T_{\nu_\alpha}/T_\gamma)^3$, when e^+e^- pairs annihilate into photons. The corresponding contribution of neutrinos in equilibrium to the total energy density, usually parameterized as $\rho_r/\rho_\gamma = 1 + \frac{7}{8} (\frac{4}{11})^{4/3} N_{\text{eff}}$ after the e^+e^- annihilation phase, is enhanced for non-zero neutrino asymmetries as follows

$$N_{\text{eff}} = 3 + \sum_{\alpha=e,\mu,\tau} \left[\frac{30}{7} \left(\frac{\xi_\alpha}{\pi} \right)^2 + \frac{15}{7} \left(\frac{\xi_\alpha}{\pi} \right)^4 \right]. \quad (3)$$

The parameter N_{eff} is the *effective number of neutrinos* whose standard value is 3 in the limit of instantaneous neutrino decoupling.

We are interested in calculating the evolution of the active neutrino spectra from large temperatures, when they followed a Fermi–Dirac form, until the BBN epoch. This includes taking into account neutrino interactions among themselves and with charged leptons, as well as flavor oscillations, which become effective at similar temperatures. In such a case the best way to describe neutrino distributions is to use matrices in flavor space $\varrho_{\mathbf{p}}$ [24,25]. For three active neutrino species, we need 3×3 matrices in flavor space $\varrho_{\mathbf{p}}$ for each neutrino momentum \mathbf{p} , where the diagonal elements are the usual occupation numbers and the off-diagonal ones encode phase information and vanish for zero mixing. The corresponding equations of motion (EOMs) for $\varrho_{\mathbf{p}}$ are the same as those considered in Refs. [22,23], where the reader can find more details on the approximations made to solve them and related references,

$$i \frac{d\varrho_{\mathbf{p}}}{dt} = [\Omega_{\mathbf{p}}, \varrho_{\mathbf{p}}] + C[\varrho_{\mathbf{p}}, \bar{\varrho}_{\mathbf{p}}], \quad (4)$$

and similar for the antineutrino matrices $\bar{\varrho}_{\mathbf{p}}$. The last term corresponds to the effect of neutrino collisions, i.e. interactions with exchange of momenta, which are implemented as in Ref. [22]. These collision terms, proportional to the square of the Fermi constant G_F , are crucial for modifying the neutrino distributions to achieve equilibrium with e^\pm and, indirectly, with photons. In the absence of neutrino mixing, the EOMs include only collision terms and preserve the flavour neutrino asymmetries η_{ν_α} .

The first term on the right-hand side of Eq. (4) describes flavor oscillations,

$$\Omega_{\mathbf{p}} = \frac{M^2}{2p} + \sqrt{2} G_F \left(-\frac{8p}{3m_W^2} E + \varrho - \bar{\varrho} \right), \quad (5)$$

where $p = |\mathbf{p}|$ and M is the neutrino mass matrix (opposite sign for antineutrinos), which in the flavour basis is not diagonal and includes the mixing parameters that characterizes the vacuum term of oscillations. In our calculations we have fixed both mass-squared differences and the angles θ_{12} and θ_{23} to the best-fit values in [3]. Varying these parameters within the allowed 3σ ranges does not modify our results. Instead, we will consider the whole presently allowed range of θ_{13} values, approximately from 0.001 to 0.035–0.05 at 3σ (depending on the reactor neutrino fluxes, see [2,3]), adding the case of zero θ_{13} for comparison.

Matter effects are included via the term proportional to the Fermi constant G_F , the so-called neutrino potentials. The one proportional to $\varrho - \bar{\varrho}$, where $\varrho = \int \varrho_{\mathbf{p}} d^3\mathbf{p}/(2\pi)^3$ (and similar for antineutrinos) arises from neutrino–neutrino interactions and it was shown in [18–20] that for the relevant values of neutrino asymmetries this matter term dominates but does not suppress flavour oscillations. Instead, this term leads to synchronized oscillations of neutrinos and antineutrinos of different momenta [26].

The small baryon density in the early Universe implies that the refractive matter term proportional to the difference between the charged lepton and antilepton number densities (CP asymmetric) can be neglected compared to the CP symmetric term, proportional to the sum of energy densities [24,27]. This appears in Eq. (4) with E , the 3×3 flavor diagonal matrix of charged-lepton energy densities. The onset of flavour oscillations occurs at a temperature at which the vacuum and charged-leptons background terms become equal in magnitude, i.e. when the following terms

$$-\frac{\Delta m^2}{2p} \cos 2\theta, \quad -\frac{8\sqrt{2}G_F p}{3m_W^2} (\rho_{l^-} + \rho_{l^+}) \quad (6)$$

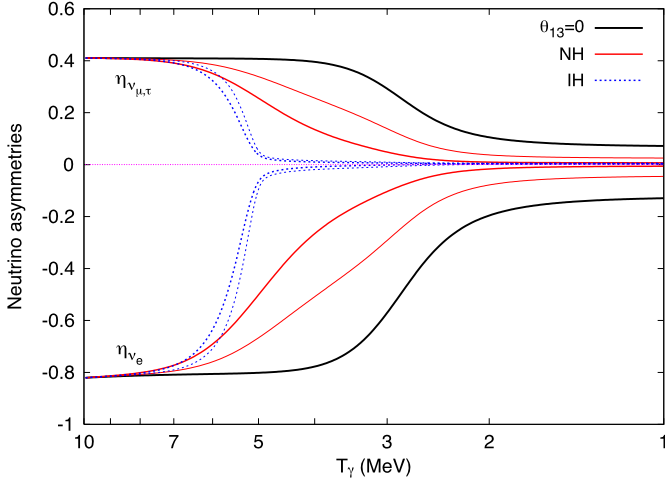


Fig. 1. Evolution of the flavor neutrino asymmetries when $\eta_{\nu_e}^{\text{in}} = -0.82$ and zero total asymmetry. The outer solid curves correspond to vanishing θ_{13} (black lines), while the inner ones (red lines) were calculated in the NH for two values of $\sin^2 \theta_{13}$: from left to right, 0.04 and 0.02. The same two values of $\sin^2 \theta_{13}$ apply to the cases shown as blue dotted lines, but in the IH. (For interpretation of the references to color in this figure legend, the reader is referred to the web version of this Letter.)

are comparable for the relevant mixing parameters Δm^2 and θ , and the charged-lepton energy density ρ_l (see e.g. [19]). Tau leptons are too heavy to have a significant density at MeV temperatures, while the energy density of μ^\pm is exponentially suppressed, leading to $\nu_\tau - \nu_\mu$ mixing driven by Δm_{31}^2 and θ_{23} at $T \simeq 15$ MeV [18], when weak interactions are fully effective. Thus, as in previous works, our numerical calculations start at $T = 10$ MeV with initial degeneracy parameters $\xi_x \equiv \xi_\mu = \xi_\tau$ and ξ_e .

For flavour neutrino oscillations involving ν_e 's, the crucial parameters are Δm_{31}^2 and θ_{13} because they fix the moment when the neutrino conversions become important, i.e. when the absolute values of both terms in Eq. (6) are equal. One easily finds that this occurs at a temperature

$$T_c \simeq 19.9 \left(\frac{p}{T} \right)^{-1/3} \left(\frac{|\Delta m_{31}^2|}{\text{eV}^2} \right)^{1/6} \text{ MeV} \quad (7)$$

for $\cos 2\theta_{13} \simeq 1$ and e^\pm taken as relativistic particles. For $|\Delta m_{31}^2| = 2.5 \times 10^{-3} \text{ eV}^2$ and an average neutrino momentum, one finds $T_c \simeq 5$ MeV. If $\Delta m_{31}^2 > 0$ (normal neutrino mass hierarchy, NH) both terms in Eq. (6) have the same sign and neutrino oscillations follow an MSW conversion when the vacuum term overcomes the matter potential at $T \simeq T_c$. The degree of conversion depends in this case on the value of θ_{13} [18–20], being very efficient compared with $\theta_{13} = 0$ if this mixing angle presents a value close to the upper bound, as can be seen in Fig. 1 for one particular case with zero total lepton number and different choices of θ_{13} .

The conversion for non-zero θ_{13} is more evident for the inverted mass hierarchy, as shown in Fig. 1, due to the resonant character of the MSW transition for $\Delta m_{31}^2 < 0$. Indeed, for IH the sum of the two terms in Eq. (6) vanishes and the equipartition of the total lepton asymmetry among the three neutrino flavours is quickly achieved, even for $\sin^2 \theta_{13} \lesssim 0.01$, unless of course θ_{13} is extremely small. Finally, for negligible θ_{13} flavour oscillations are not effective until $T \lesssim 3$ MeV (outer lines in Fig. 1), a value that can be found substituting Δm_{31}^2 for $\Delta m_{21}^2 = 7.6 \times 10^{-5} \text{ eV}^2$ in Eq. (6).

The moment when flavour oscillations in the presence of neutrino asymmetries become effective is important not only to establish the electron neutrino asymmetry at the onset of BBN, but also to determine whether weak interactions with e^+e^- can still

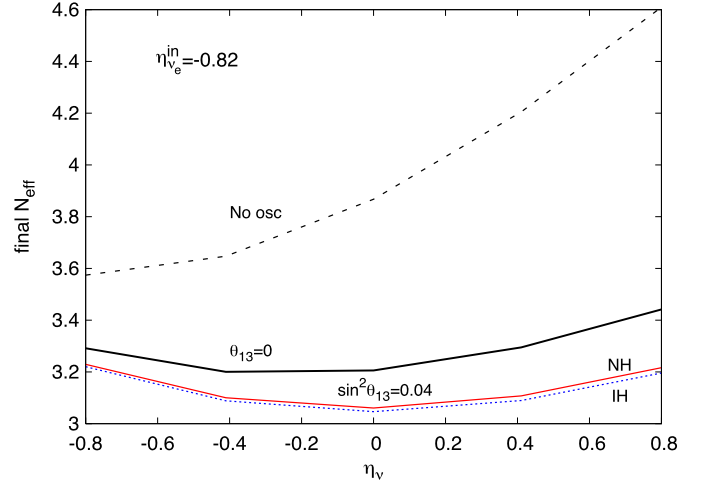


Fig. 2. Final contribution of neutrinos to the total radiation energy density, parametrized with N_{eff} , as a function of the total neutrino asymmetry for a particular value of the initial electron neutrino asymmetry ($\eta_{\nu_e}^{\text{in}} = -0.82$). From top to bottom, the various lines correspond, respectively, to the following cases: no neutrino oscillations (η_{ν_e} conserved), $\theta_{13} = 0$, and $\sin^2 \theta_{13} = 0.04$ for normal (red solid line) and inverted (blue dotted line) neutrino mass hierarchy. (For interpretation of the references to color in this figure legend, the reader is referred to the web version of this Letter.)

keep neutrinos in good thermal contact with the ambient plasma. Oscillations redistribute the asymmetries among the flavours, but only if they occur early enough would interactions preserve Fermi–Dirac spectra for neutrinos, in such a way that a chemical potential μ_{ν_α} is well defined for each η_{ν_α} and the relations in Eqs. (2) and (3) remain valid. For instance, if the initial values of the flavour asymmetries have opposite signs, neutrino conversions will tend to reduce the asymmetries which in turn will decrease N_{eff} . But if flavour oscillations take place at temperatures close to neutrino decoupling, this would not hold and an extra contribution of neutrinos to radiation is expected with respect to the value in Eq. (3), as emphasized in [22].

A way to see the role of flavour oscillations on the reduction of the final value of N_{eff} from neutrino asymmetries is given in Fig. 2. Here we have fixed the initial electron neutrino asymmetry to $\eta_{\nu_e}^{\text{in}} = -0.82$ as in Fig. 1, but varied the total asymmetry in the range $-0.8 \leq \eta_\nu \leq 0.8$. In the absence of neutrino mixing the final value of N_{eff} is that given by Eq. (3), directly related to the chemical potentials, and for this particular range it can be as large as $N_{\text{eff}} \simeq 4.6$. Instead, when oscillations are included the three flavour asymmetries are modified and the contribution of neutrinos is largely reduced, even for $\theta_{13} = 0$. Finally, for $\sin^2 \theta_{13} = 0.04$ and both NH or IH, the final flavour asymmetries are given by $\eta_{\nu_\alpha} \simeq \eta_\nu/3$. In such a case, we expect neutrinos to almost follow Fermi–Dirac spectra and N_{eff} as given in Eq. (3). For instance, for $\eta_\nu = 0.8$ one expects $\xi_{\nu_e, \mu, \tau} \simeq 0.38$ and a total contribution to the radiation energy density of $N_{\text{eff}} \simeq 3.19$, very close to what we find in our numerical calculations for $\sin^2 \theta_{13} = 0.04$, while we found $N_{\text{eff}} \simeq 3.43$ for $\theta_{13} = 0$.

3. BBN bounds on the cosmological lepton asymmetry

Cosmological neutrinos influence the primordial production of light elements in two ways. First of all, they contribute to the radiation energy density that fixes the expansion of the Universe during BBN, a background effect that is parameterized with N_{eff} . For the particular case of ${}^4\text{He}$, its primordial abundance is enhanced for $N_{\text{eff}} > 3$, as in the case of neutrino asymmetries. On the other hand, electron neutrinos and antineutrinos are involved in

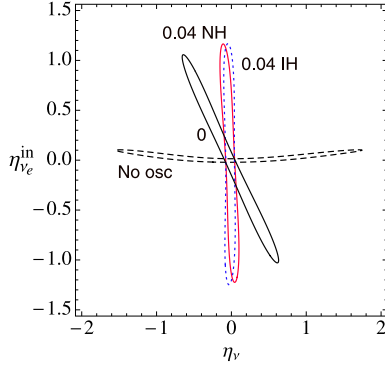


Fig. 3. 95% C.L. contours from our BBN analysis in the η_ν - $\eta_{\nu_e}^{\text{in}}$ plane for several values of $\sin^2 \theta_{13}$: 0 (black solid line), 0.04 and NH (red solid line), 0.04 and IH (blue dotted line). The case of no neutrino flavour oscillations is shown for comparison as the black dashed contour. (For interpretation of the references to color in this figure legend, the reader is referred to the web version of this Letter.)

the charged current weak processes which rule the neutron/proton chemical equilibrium. Thus any change in the ν_e or $\bar{\nu}_e$ momentum distribution can shift the neutron/proton ratio freeze out temperature and in turn modify the primordial ${}^4\text{He}$ abundance. This is what happens for a non-zero ν_e - $\bar{\nu}_e$ asymmetry at BBN, that shifts the neutron fraction towards larger or smaller values for negative or positive values of η_{ν_e} , respectively.

We have performed an analysis of the effects of flavour neutrino asymmetries on the BBN outcome in a similar way as in [23]. We have solved the EOMs described in the previous section in a wide range of values for the total lepton (neutrino) asymmetry η_ν , unchanged by oscillations, and the initial electron neutrino asymmetry $\eta_{\nu_e}^{\text{in}}$. The obtained time-dependent neutrino distributions are then used as an input for the public numerical code `PARTHENOSPE` [28,29], as described in [23]. The computed abundances of both the ratio ${}^2\text{H}/\text{H}$ and the ${}^4\text{He}$ mass fraction, Y_p , are compared with the corresponding experimental determinations in order to find the allowed region of asymmetries η_ν and $\eta_{\nu_e}^{\text{in}}$. Here, as in [23], we consider for the primordial ${}^2\text{H}$ abundance the value

$${}^2\text{H}/\text{H} = (2.87 \pm 0.22) \times 10^{-5}, \quad (8)$$

obtained by averaging seven determinations from different Quasar Absorption Systems [30]. For the ${}^4\text{He}$ mass fraction we use, as a conservative value, the result of the data collection analysis performed in [30],

$$Y_p = 0.250 \pm 0.003. \quad (9)$$

The main results of our BBN analysis are shown in Fig. 3 for the adopted determinations of ${}^2\text{H}$ and ${}^4\text{He}$. From this plot one can easily see the effect of flavour oscillations on the BBN constraints on the total neutrino asymmetry. In the absence of neutrino mixing the value of η_{ν_e} is severely constrained by ${}^4\text{He}$ data, arising from a narrow region for the electron neutrino degeneracy, $-0.018 \leq \xi_e \leq 0.008$ at 68% C.L. Instead, the asymmetry for other neutrino flavours could be much larger, since the absolute value of total asymmetry is only restricted to the region $|\eta_\nu| \lesssim 2.6$ [16, 17]. As we have previously seen, flavour oscillations modify this picture and an initially large $\eta_{\nu_e}^{\text{in}}$ can be compensated by an asymmetry in the other flavours with opposite sign. The most restrictive BBN bound on η_{ν_e} applies then to the total asymmetry, an effect that can be seen graphically in Fig. 3 as a *rotation* of the allowed region from a quasi-horizontal one for zero mixing to an almost vertical region for $\sin^2 \theta_{13} = 0.04$, in particular for the IH. In all cases depicted in Fig. 3 the allowed values of the asymmetries are mainly fixed by the ${}^4\text{He}$ bound, which imposes that the value of

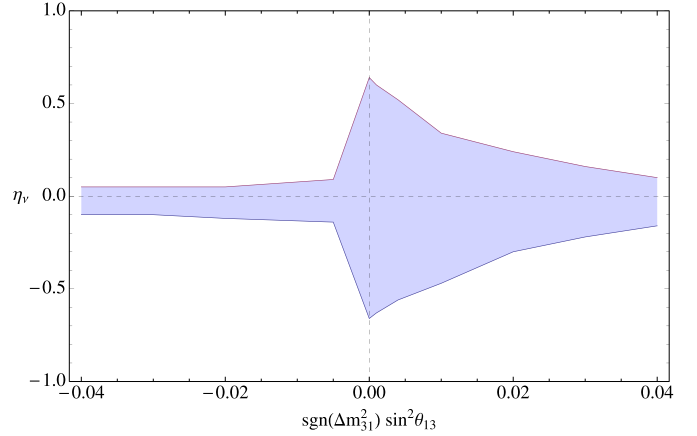


Fig. 4. The shadowed region corresponds to the values of the total neutrino asymmetry compatible with BBN at 95% C.L., as a function of θ_{13} and the neutrino mass hierarchy.

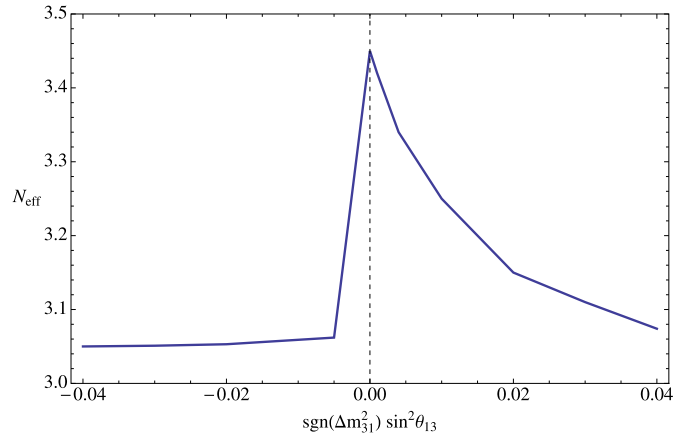


Fig. 5. Largest values of N_{eff} from primordial neutrino asymmetries compatible with BBN at 95% C.L., as a function of θ_{13} and the neutrino mass hierarchy.

η_{ν_e} at BBN must be very close to zero, while the data on primordial deuterium is crucial for closing the region.

For values of θ_{13} close to the upper limits set by experimental data, the combined effect of oscillations and collisions leads to an efficient mixing of all neutrino flavours before BBN. Therefore, the individual neutrino asymmetries have similar values, approximately $\eta_{\nu_\alpha} \simeq \eta_\nu/3$, and the BBN bound on the electron neutrino asymmetry applies to all flavours, and in turn to η_ν as considered in previous analyses [30–36]. We find that for $\sin^2 \theta_{13} = 0.04$ the allowed region at 95% C.L. is $-0.17(-0.1) \leq \eta_\nu \leq 0.1(0.05)$ for neutrino masses following a normal (inverted) mass hierarchy. Note, however, that in the IH this result approximately holds for any value of $\sin^2 \theta_{13}$ within the favoured region by oscillation data, due to the resonant character of the conversions. Instead, as discussed in [23], in the NH even values of order $|\eta_\nu| \simeq 0.6$ are still compatible with BBN if θ_{13} is very small. The allowed regions of the total neutrino asymmetry are depicted in Fig. 4 as a function of the mixing angle θ_{13} and the mass hierarchy.

Finally, the dependence of the largest value of N_{eff} from neutrino asymmetries in the region compatible with BBN, as a function of the neutrino mass hierarchy and the mixing angle θ_{13} is reported in Fig. 5. If the true value of θ_{13} lies in the upper part of the region favoured by oscillation experiments (in particular T2K) or $\Delta m_{31}^2 < 0$, the presence of primordial asymmetries cannot lead to a contribution to the radiation energy density $N_{\text{eff}} > 3.1$. On the

other hand, for the NH and very small values of θ_{13} , larger values of N_{eff} are still compatible with BBN data, up to 3.43 at 95% C.L.

4. Conclusions

We have found the BBN constraints on the cosmological lepton number and its associated contribution to the radiation energy density, taking into account the effect of flavour neutrino oscillations. Once the other neutrino mixing parameters have been fixed by oscillation data, we have shown that pinpointing the value of θ_{13} is crucial to establish the degree of conversion of flavour neutrino asymmetries in the early Universe.

We conclude that the most stringent BBN bound on the total neutrino asymmetry, $|\eta_\nu| \lesssim 0.1$, requires that reactor neutrino experiments in the near future [37], such as Double Chooz, Daya Bay or Reno, confirm that the value of the third neutrino mixing angle is such that $\sin^2 \theta_{13} \gtrsim 0.03$. This conclusion also applies to the whole allowed range of θ_{13} values at 3σ [2,3] if neutrino masses follow an inverted hierarchy scheme. For smaller values of this mixing angle in the NH the BBN bound is relaxed, up to a maximum allowed range of $-0.7 \lesssim \eta_\nu \lesssim 0.6$ for $\theta_{13} = 0$.

Similarly, a measured value $\sin^2 \theta_{13} \gtrsim 0.03$ will imply that the maximum contribution of neutrino asymmetries to the radiation content of the Universe cannot exceed $N_{\text{eff}} \simeq 3.1$, well below the expected sensitivity of the Planck satellite (0.4 at 2σ) [38–40], whose first data release on the anisotropies of the cosmic microwave background (CMB) is expected in one year or so.

Finally, we emphasize that BBN remains the best way to constrain a potential cosmological lepton number, despite the present precision of the measurements of the CMB anisotropies and other late cosmological observables. Bounds on the neutrino asymmetries with these data [41–44] do not improve those found in our work, but are of course sensitive to other neutrino properties such as their masses.

Acknowledgements

G. Mangano, G. Miele, O. Pisanti and S. Sarikas acknowledge support by the Istituto Nazionale di Fisica Nucleare I.S. FA51 and the PRIN 2010 “Fisica Astroparticellare: Neutrini ed Universo Primordiale” of the Italian Ministero dell’Istruzione, Università e Ricerca. S. Pastor was supported by the Spanish grants FPA2008-00319, FPA2011-22975 and Multidark CSD2009-00064 (MICINN) and PROMETEO/2009/091 (Generalitat Valenciana), and by the EC contract UNILHC PITN-GA-2009-237920. This research was also supported by a Spanish–Italian MICINN–INFN agreement, refs. ACI2009-1051 and AIC10-D-000543.

References

- [1] T. Schwetz, M.A. Tortola, J.W.F. Valle, *New J. Phys.* 13 (2011) 063004, arXiv:1103.0734.
- [2] G.L. Fogli, E. Lisi, A. Marrone, A. Palazzo, A.M. Rotunno, *Phys. Rev. D* 84 (2011) 053007, arXiv:1106.6028.
- [3] T. Schwetz, M.A. Tortola, J.W.F. Valle, *New J. Phys.* 13 (2011) 109401, arXiv:1108.1376.
- [4] K. Abe, et al., T2K Collaboration, *Phys. Rev. Lett.* 107 (2011) 041801, arXiv:1106.2822.
- [5] H. Nunokawa, S.J. Parke, J.W.F. Valle, *Prog. Part. Nucl. Phys.* 60 (2008) 338, arXiv:0710.0554.
- [6] G. Mangano, G. Miele, S. Pastor, T. Pinto, O. Pisanti, P.D. Serpico, *Nucl. Phys. B* 729 (2005) 221, arXiv:hep-ph/0506164.
- [7] A.D. Dolgov, F.L. Villante, *Nucl. Phys. B* 679 (2004) 261, arXiv:hep-ph/0308083.
- [8] D.P. Kirilova, M.P. Panayotova, *JCAP* 0612 (2006) 014, arXiv:astro-ph/0608103.
- [9] A. Melchiorri, O. Mena, S. Palomares-Ruiz, S. Pascoli, A. Slosar, M. Sorel, *JCAP* 0901 (2009) 036, arXiv:0810.5133.
- [10] J. Hamann, S. Hannestad, G.G. Raffelt, Y.Y.Y. Wong, *JCAP* 1109 (2011) 034, arXiv:1108.4136.
- [11] E. Komatsu, et al., *Astrophys. J. Suppl. Ser.* 192 (2011) 18, arXiv:1001.4538.
- [12] J. March-Russell, H. Murayama, A. Riotto, *JHEP* 9911 (1999) 015, hep-ph/9908396.
- [13] J. McDonald, *Phys. Rev. Lett.* 84 (2000) 4798, hep-ph/9908300.
- [14] D.J. Schwarz, M. Stuke, *JCAP* 0911 (2009) 025, arXiv:0906.3434.
- [15] V.B. Semikoz, D.D. Sokoloff, J.W.F. Valle, *Phys. Rev. D* 80 (2009) 083510, arXiv:0905.3365.
- [16] H.S. Kang, G. Steigman, *Nucl. Phys. B* 372 (1992) 494.
- [17] S.H. Hansen, G. Mangano, A. Melchiorri, G. Miele, O. Pisanti, *Phys. Rev. D* 65 (2002) 023511, arXiv:astro-ph/0105385.
- [18] A.D. Dolgov, S.H. Hansen, S. Pastor, S.T. Petcov, G.G. Raffelt, D.V. Semikoz, *Nucl. Phys. B* 632 (2002) 363, arXiv:hep-ph/0201287.
- [19] Y.Y.Y. Wong, *Phys. Rev. D* 66 (2002) 025015, arXiv:hep-ph/0203180.
- [20] K.N. Abazajian, J.F. Beacom, N.F. Bell, *Phys. Rev. D* 66 (2002) 013008, arXiv:astro-ph/0203442.
- [21] C. Lunardini, A.Yu. Smirnov, *Phys. Rev. D* 64 (2001) 073006, arXiv:hep-ph/0012056.
- [22] S. Pastor, T. Pinto, G.G. Raffelt, *Phys. Rev. Lett.* 102 (2009) 241302, arXiv:0808.3137.
- [23] G. Mangano, G. Miele, S. Pastor, O. Pisanti, S. Sarikas, *JCAP* 1103 (2011) 035, arXiv:1011.0916.
- [24] G. Sigl, G. Raffelt, *Nucl. Phys. B* 406 (1993) 423.
- [25] B.H. McKellar, M.J. Thomson, *Phys. Rev. D* 49 (1994) 2710.
- [26] S. Pastor, G.G. Raffelt, D.V. Semikoz, *Phys. Rev. D* 65 (2002) 053011, arXiv:hep-ph/0109035.
- [27] D. Nötzold, G. Raffelt, *Nucl. Phys. B* 307 (1988) 924.
- [28] O. Pisanti, A. Cirillo, S. Esposito, F. Iocco, G. Mangano, G. Miele, P.D. Serpico, *Comput. Phys. Comm.* 178 (2008) 956, arXiv:0705.0290.
- [29] PArthENoPE web page: <http://parthenope.na.infn.it/>.
- [30] F. Iocco, G. Mangano, G. Miele, O. Pisanti, P.D. Serpico, *Phys. Rep.* 472 (2009) 1, arXiv:0809.0631.
- [31] V. Barger, J.P. Kneller, H.S. Lee, D. Marfatia, G. Steigman, *Phys. Lett. B* 566 (2003) 8, arXiv:hep-ph/0305075.
- [32] V. Barger, J.P. Kneller, P. Langacker, D. Marfatia, G. Steigman, *Phys. Lett. B* 569 (2003) 123, arXiv:hep-ph/0306061.
- [33] A. Cuoco, F. Iocco, G. Mangano, G. Miele, O. Pisanti, P.D. Serpico, *Int. J. Mod. Phys. A* 19 (2004) 4431, arXiv:astro-ph/0307213.
- [34] R.H. Cyburt, B.D. Fields, K.A. Olive, E. Skillman, *Astropart. Phys.* 23 (2005) 313, arXiv:astro-ph/0408033.
- [35] P.D. Serpico, G.G. Raffelt, *Phys. Rev. D* 71 (2005) 127301, arXiv:astro-ph/0506162.
- [36] V. Simha, G. Steigman, *JCAP* 0808 (2008) 011, arXiv:0806.0179.
- [37] P. Huber, M. Lindner, M. Rolinec, T. Schwetz, W. Winter, *Phys. Rev. D* 70 (2004) 073014, arXiv:hep-ph/0403068.
- [38] R. Bowen, S.H. Hansen, A. Melchiorri, J. Silk, R. Trotta, *Mon. Not. Roy. Astron. Soc.* 334 (2002) 760, arXiv:astro-ph/0110636.
- [39] S. Bashinsky, U. Seljak, *Phys. Rev. D* 69 (2004) 083002, arXiv:astro-ph/0310198.
- [40] J. Hamann, S. Hannestad, J. Lesgourgues, C. Rampf, Y.Y.Y. Wong, *JCAP* 1007 (2010) 022, arXiv:1003.3999.
- [41] J. Hamann, J. Lesgourgues, G. Mangano, *JCAP* 0803 (2008) 004, arXiv:0712.2826.
- [42] L.A. Popa, A. Vasile, *JCAP* 0806 (2008) 028, arXiv:0804.2971.
- [43] M. Shiraishi, K. Ichikawa, K. Ichiki, N. Sugiyama, M. Yamaguchi, *JCAP* 0907 (2009) 005, arXiv:0904.4396.
- [44] E. Castorina, et al., in preparation.